J. Fluid Mech. (1965), *vol.* 21, *part* 2, *pp.* 281–303
Printed in Great Britain

Ignition and extinction in combustion of initially unmixed reactants

By FRANCIS E. FENDELL
Office of Research, Aerospace Corp., San Bernardino, California

(Received 18 June 1964)

The adequacy of direct one-step chemical kinetics for describing ignition and extinction in initially unmixed gases is studied through the particular case of inviscid axisymmetric stagnation-point flow. Oxidant is assumed to blow from upstream infinity at a non-gaseous reservoir of pure fuel at its boiling (or subliming) temperature. Before reaching the reservoir the oxidant reacts with gaseous fuel flowing in the opposite direction to form product and release heat. This heat is in part conducted and diffused to the reservoir interface to transform more fuel into the gaseous state and continue the steady-state burning. Second-order Arrhenius kinetics for Lewis-number unity is examined. A critical parameter characterizing the phenomenon is shown to be the first Damkohler similarity group D_1, the ratio of a time characterizing the flow to a time characterizing the chemical activity.

For small D_1 the reactants convect away heat without releasing the energy stored in their chemical bonds. Regular perturbation about chemically frozen flow establishes this condition as the weak burning limit. For large D_1 singular perturbation describes a narrow region of intense chemical activity. For infinite D_1 (indefinitely fast rate of reaction) the region is reduced to a surface of discontinuity (the thin-flame kinetics of Burke & Schumann).

For intermediate D_1 numerical techniques establish that a solution describing burning of moderate intensity joins the two previously mentioned asymptotic limits. It is suggested that sudden transition of the system between the various branches in this domain of intermediate D_1 accounts for the phenomena of ignition and extinction of burning.

1. Introduction

Burning may be categorized as involving either a homogeneous mixture of reactants combined before combustion, or a reaction between initially unmixed reactants that combine at the flame. Only slow burning is possible in the unpremixed case, to be studied here, because only those fuel molecules at the flame region are accessible to oxidant molecules. For unpremixed gases classical one-component analysis is inadequate—a complete description involves recognition of the multicomponent nature of the flow. Diffusion then joins the entropy-producing mechanisms of heat conduction and viscosity.

'Flame' is used in the general sense of a region where appreciable chemical reaction occurs. The geometry, temperatures, and properties of gases to be

studied render radiation negligible. Furthermore, attention is confined to homogeneous kinetics in the gaseous phase because the two-phase interface is at too low a temperature and accessible to too small a fraction of the oxidant for appreciable reaction to occur there.

In most treatments of chemically reacting flows, discussion centres around two opposing limits: (1) frozen flow for zero rate of reaction, and (2) equilibrium flow for infinite rate of reaction. The frozen limit refers to conditions in which the time for a reaction-inducing collision to occur is much longer than the time for an element of reactant to flow through the flame. Virtually no creation or destruction of a species occurs so the chemical terms vanish. For unpremixed flow in which the rate of reaction is infinite and in which reaction can proceed in only one direction, chemical equilibrium cannot be set up until the gases come into physical contact. Then they instantaneously react on the surface of contact to form an indefinitely thin region of chemical activity. Intuitively, in the steady state the interface of contact will lie at points in the flow at which the gases meet in stoichiometric proportion so that the reaction goes to immediate completion. For finite rates of reaction the details of the chemical kinetics must be specified.

2. Equations

If the model of independent co-existent continua, each obeying the laws of dynamics and thermodynamics, is adopted, then a complete Eulerian description would involve solution of the following equations:

$$\nabla.(\rho\mathbf{v}) = 0, \tag{2.1}$$

$$\rho\mathbf{v}.\nabla\mathbf{v} = -\nabla P, \tag{2.2}$$

$$\rho\mathbf{v}.\nabla Y_K - \nabla.(\rho D\nabla Y_K) = \omega_K \quad (K = 1, 2, \ldots, n), \tag{2.3}$$

$$\rho\mathbf{v}.\nabla(C_P T) - \nabla.(\lambda\nabla T) = -\sum_K h_0^K \omega_K, \tag{2.4}$$

plus an equation of state.† Here $\mathbf{v}$ is the velocity vector, T the temperature, ρ the density and P the pressure of the gas. The heat flux has been taken as linearly proportional to temperature gradient, λ being the proportionality factor. Similarly, the diffusional velocity of species K has been taken linearly proportional to gradient of mass fraction of species K, Y_K. Here the proportionality factor D, sometimes referred to as the mass transfer coefficient, has been taken as universal for the n species present. The mass fraction $Y_K = \rho_K/\rho$, where ρ_K is the density of species k and $\rho = \sum_K \rho_K$. It can be shown (Fendell 1964) that equations (2.1)–(2.4) can describe a wide range of steady flows in the absence of body forces, in which thermal effects are pronounced but the dynamics are approximately those of a non-reacting gas at large Reynolds number but small Eckert number ($|\mathbf{v}|^2/C_P T$). The Schmidt number of the gas ($\mu/\rho D$) is order unity and the Peclet number of the flow ($\rho|\mathbf{v}|C_P L/\lambda$, where L is a typical length) not very large. The enthalpy of formation at temperature T_0 is h_0^K and is taken to be

† A list of symbols is given at the end of this article. In this connection see also Nachbar, Williams & Penner (1959).

the dominant portion of the enthalpy of any species K, assumed expressible as $C_P^K(T-T_0)+h_0^K$. The net heat capacity at constant pressure $C_P = \sum_K C_P^K Y_K$. The net production of mass of species K per unit time ω_K is in general a non-linear function of the temperature T and mass fractions Y_K.

Equations (2.1) and (2.2) are the familiar Euler equations representing global (i.e. net over-all-species) conservation of mass and linear momentum. Equation (2.4) is the global conservation of energy, in which convective and conductive transport of thermal energy appears along with the heat released by chemical reaction, here taken as exothermic. Equations (2.3) represent conservation of mass for each of the n independent species present: convection and diffusive transport of mass appears along with the source-sink-like effect of chemical reaction.

3. Approximations

In aerothermochemical problems solution is usually attained by separating the dynamics from the thermodynamics. The only rigorous means of separation for the stagnation-region flow is by adopting $\rho = \text{const.}$ as the equation of state; this should not compromise the fundamental physics. It is consistent to adopt constant values for the transport coefficients.

The adoption of direct chemical reaction between the initial reactants should roughly reproduce the net effect of many simultaneous reactions involving intermediates. By definition

$$\omega_K = m_K(dM_K/dt),$$

where m_K is the molecular weight of species K and M_K the molar concentration. If the direct reaction is represented by

$$\sum_{K=1}^{n} (\nu_1^K - \nu_2^K) m_K = 0,$$

where ν_1^K is the stoichiometric coefficient of the reactant K and ν_2^K, of the product K, then

$$dM_K/dt = (\nu_2^K - \nu_1^K)\,(\text{r.r.})$$

where (r.r.) = the rate of reaction. Further, if

$$(\alpha_K)^{-1} = -(\nu_2^K - \nu_1^K) m_K/m, \quad \text{where} \quad m = \sum_K \nu_1^K m_K = \sum_K \nu_2^K m_K$$

and $\Delta H_c = \sum_K m_K h_0^K(\nu_1^K - \nu_2^K) =$ specific heat released through combustion, and if $\overline{Y}_K = \alpha_K Y_K$, then equations (2.3) and (2.4) become

$$(\mathbf{v}.\nabla - D\nabla^2)\overline{Y}_K = -m(\text{r.r.})/\rho \quad (K = 1, 2, \ldots, n), \tag{3.1}$$

$$(\mathbf{v}.\nabla - \chi\nabla^2)T = \Delta H_c(\text{r.r.})/\rho C_P, \tag{3.2}$$

where C_P has been taken as constant, and $\chi = \lambda/\rho C_P$.

If the inviscid incompressible flow problem can be solved, then $\mathbf{v}$ serves as a variable coefficient in the remaining equations (3.1) and (3.2), in which all the non-linearities are confined to the rate of reaction (r.r.). Schvab and Zeldovitch

(see Zeldovitch 1951) were the first to notice $2n$ integrals of the $(2n+2)$ remaining could be found from solution of a convection-diffusion balance if $D = \chi$. In the literature this step is described as taking the Lewis–Semenov number, $Le = D/\chi$, as unity and is in general a good approximation provided no component of the n present has a molecular weight significantly lower than the other species present (for air $Le \approx 1.4$ until high temperatures). The equations (3.1) and (3.2) are then, for example

$$(\mathbf{v}.\nabla - \chi\nabla^2)(\overline{Y}_K + mC_P T/\Delta H_C) = 0 \quad (K = 1, 2, \ldots, n), \tag{3.3}$$

$$(\mathbf{v}.\nabla - \chi\nabla^2)T = \Delta H_C(\text{r.r.})/\rho C_P. \tag{3.4}$$

4. Axisymmetric geometry

For axisymmetric flow without swirl under $\rho = \text{const.}$, the governing set (2.1), (2.2), (3.1), and (3.2) becomes in terms of cylindrical-polar co-ordinates (r, θ, z) with velocity components (u, o, w):

$$\partial(ur)/\partial r + \partial(rw)/\partial z = 0, \tag{4.1}$$

$$Lu = -\rho^{-1}\,\partial P/\partial r, \tag{4.2}$$

$$Lw = -\rho^{-1}\,\partial P/\partial z, \tag{4.3}$$

$$LT = \chi\left[\frac{\partial^2 T}{\partial z^2} + \frac{1}{r}\frac{\partial}{\partial r}\left(r\frac{\partial T}{\partial r}\right)\right] + \frac{\Delta H_C(\text{r.r.})}{\rho C_P}, \tag{4.4}$$

$$L\overline{Y}_K = \chi\left[\frac{\partial^2 \overline{Y}_K}{\partial z^2} + \frac{1}{r}\frac{\partial}{\partial r}\left(r\frac{\partial \overline{Y}_K}{\partial r}\right)\right] - \frac{m(\text{r.r.})}{\rho}, \tag{4.5}$$

where $L = u(\partial/\partial r) + w(\partial/\partial z)$.

The geometrical arrangement is given in figure 1. For $-\infty \leqslant z \leqslant z_w$ there is a reservoir of pure liquid (or solid) fuel uniformly at its normal boiling (or sublimation) temperature. The reservoir interface will henceforth be called the wall and denoted z_w. For a direct unopposed reaction it is incompatible to demand that the reservoir be pure fuel at its boiling temperature; the Clausius–Chapeyron equation should be allowed to establish what the interface temperature is. The error in adopting the boiling temperature—a great analytic convenience—can be shown to be slight except when virtually no reaction occurs (Fendell 1964) and then there exists pure diffusive convection, an extensively studied phenomenon. As a result of the approximation it will be necessary to maintain the upstream oxidant temperature above the fuel boiling temperature for a physically meaningful solution to exist in the nearly frozen limit. This requirement is plausible, for if it is demanded that the wall temperature be maintained at a boiling level without the availability of heat from reaction, the only possible means of realizing the situation in the steady state for the specified geometry is to have a hot upstream flow of oxidant.

Because oxidant is being blown downstream and fuel is moving upstream, there will occur a stagnation plane in the axisymmetric flow postulated, hence a natural origin for the z co-ordinate. Fuel must diffuse against convection for $z > 0$ and oxidant likewise for $z < 0$. Both reactants cross the stagnation plane

by diffusion only. Fresh reactants moving by diffusive and convective transport toward the flame are preheated by conduction and by diffusing products.

In the assumed absence of vortex sheets symmetry requires that the flow for all $z_w \leqslant z \leqslant 0$ be the mirror image of the inviscid incompressible axisymmetric stagnation point flow for $z \geqslant 0$. The solution to (4.1)–(4.3) is then well known to be $\mathbf{v} = \nabla x(-\psi\hat{\boldsymbol{\theta}}/r)$ where $\psi = ar^2z$ and $P/\rho = (P/\rho)_0 - \frac{1}{2}a^2(r^2+4z^2)$. $\hat{\boldsymbol{\theta}}$ is a unit vector in the azimuthal direction, $(P/\rho)_0$ an arbitrary datum, and a a geometric scale factor which gives the magnitude of the upstream blowing.

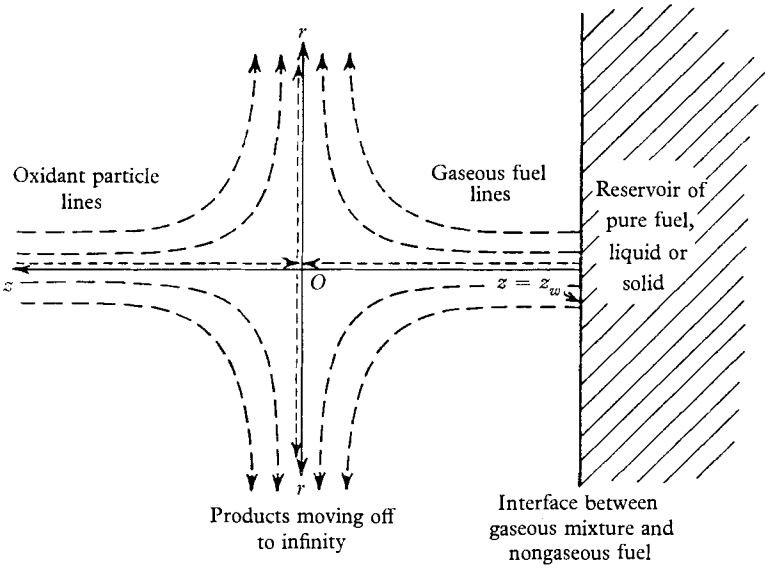

FIGURE 1. Oxidant, fuel, and product particle lines in an axially symmetric stagnation-region flow.

If equations (4.4) and (4.5) are added after substitution for u and w, and the solution sought to the resulting equation by separation of variables in the form

$$G_K(\bar{r},\bar{z}) = \overline{Y}_K + mC_PT/\Delta H_C = R(\bar{r})\,Z(\bar{z}), \tag{4.6}$$

where $\bar{r} = (a/D)^{\frac{1}{2}}r$ and $\bar{z} = (2a/D)^{\frac{1}{2}}z$, there results

$$R'' + (1/\bar{r} - \bar{r})\,R' + nR = 0, \tag{4.7}$$

in which n is a separation constant.

Since $\bar{r} = 0$ is a regular singular point, only one regular solution to (4.7) exists. If equation (4.7) is rewritten in terms of $\tilde{r} = \bar{r}/\sqrt{2}$, Hermite's equation is found for large $\bar{r}$, and only the lowest Hermite polynomial, corresponding to $n = 0$, satisfies requirements of boundedness of the remaining regular solution. Thus $\overline{Y}_K(\bar{r},\bar{z}) \to \overline{Y}_K(\bar{z})$ and $T(\bar{r},\bar{z}) \to T(\bar{z})$.

5. Chemical kinetics

Attention is now confined to the burning of fuel in oxidant so $d\mathrm{F} + b\mathrm{O} \to p\mathrm{P}$ where d, b, and p are stoichiometric coefficients. If

$$\overline{Y}_\mathrm{O} = Y_\mathrm{O}\alpha_\mathrm{O} \quad \text{where} \quad (\alpha_\mathrm{O})^{-1} = bm_\mathrm{O}/m \quad \text{and} \quad \overline{Y}_\mathrm{F} = Y_\mathrm{F}\alpha_\mathrm{F}$$

where $(\alpha_F)^{-1} = dm_F/m$ and $m = dm_F + bm_O$,

then equations (4.4) and (4.5) reduce to

$$L\overline{Y}_O = L\overline{Y}_F = -L\overline{T} = (\text{r.r.})m/2a\rho, \tag{5.1}$$

where $L = \bar{z}\,d/d\bar{z} + d^2/d\bar{z}^2$. The product mass fraction $Y_P = 1 - Y_O - Y_F$ by definition, and $\overline{T} = \Delta h_C T/\alpha_F C_P$ and $\Delta h_C = \Delta H_C/dm_F$.

Two models for the reaction rate are considered. The first uses second-order Arrhenius kinetics in which $(\text{r.r.}) = \bar{B}\rho^2 bd\overline{Y}_F\overline{Y}_O \exp(-\bar{\theta}/\overline{T})$ where $\bar{\theta}$ is the activation temperature and $\bar{B}$ the frequency factor. The other model proposed by Burke & Schumann (1928) reduces the flame to a mathematical interface across which *derivatives* of the dependent variables may be discontinuous. This flame without structure is usually expressed in terms of the following conditions:

$$\overline{Y}_O(\bar{z}_*) = \overline{Y}_F(\bar{z}_*) = 0, \tag{5.2}$$

$$\left[\frac{d\overline{T}}{d\bar{z}}\right]_{\bar{z}_{*-}}^{\bar{z}_{*+}} = \frac{d\overline{Y}_F(\bar{z}_{*-})}{d\bar{z}} = -\frac{d\overline{Y}_O(\bar{z}_{*+})}{d\bar{z}}. \tag{5.3}$$

The position of the planar thin flame is denoted by $\bar{z}_*$ and is to be found in the course of solution, along with $\overline{T}_*[= \overline{T}(\bar{z}_*)]$. Equations (5.2) and (5.3) state that the reactants meet in stoichiometric proportion and are destroyed at the thin flame, at which all mass transport is by diffusion and all heat transport by conduction.

6. Boundary-value problems

The precise relation between two boundary-value problems will be examined. The first problem employs second-order Arrhenius kinetics

$$-L\overline{T} = L\overline{Y}_F = L\overline{Y}_O = D_1\overline{Y}_O\overline{Y}_F \exp(-\bar{\theta}/\overline{T}) \quad \text{in} \quad \bar{z}_w < \bar{z} < \infty, \tag{6.1}$$

where $L = d^2/d\bar{z}^2 + \bar{z}\,d/d\bar{z}$ and

$$D_1 = \text{first Damkohler number} = \frac{\text{time characterizing flow}}{\text{time characterizing chemistry}} = \frac{\rho bd\bar{B}}{2am}. \tag{6.2}$$

For D_1 small the flow is nearly frozen and regular perturbation yields the first effects of reaction on a diffusion-convection balance (§ 8). For D_1 large a narrow region of intense reaction is surrounded upstream and downstream by diffusive convection; singular perturbation in the form of inner and outer expansions treats this asymptotic limit (§ 9). For intermediate D_1 all three effects of reaction, convection, and diffusion are important and owing to intractable non-linearities numerical integration will be used (§ 10).

The second problem examines Burke–Schumann kinetics

$$L\overline{T} = L\overline{Y}_F = L\overline{Y}_O = 0 \quad \text{in} \quad \bar{z}_w < \bar{z} < \infty, \tag{6.3}$$

except at $\bar{z} = \bar{z}_*$, where equations (5.2) and (5.3) hold. This problem is treated in § 7.

The boundary conditions for both problems are

$$\bar{z}\to\infty\colon\ \overline{T}\to\overline{T}_\infty,\quad \overline{Y}_{\mathrm{F}}\to 0,\quad \overline{Y}_{\mathrm{O}}\to(\overline{Y}_{\mathrm{O}})_\infty; \tag{6.4}$$

$$\bar{z}=\bar{z}_w\colon\ \overline{T}=\overline{T}_B, \tag{6.5}$$

$$d\overline{T}/d\bar{z}=-\alpha_{\mathrm{F}}\bar{L}\bar{z}_w, \tag{6.6}$$

$$\bar{z}_w\overline{Y}_{\mathrm{O}}+d\overline{Y}_{\mathrm{O}}/d\bar{z}=0, \tag{6.7}$$

$$\bar{z}_w(\overline{Y}_{\mathrm{F}}-\alpha_{\mathrm{F}})+d\overline{Y}_{\mathrm{F}}/d\bar{z}=0. \tag{6.8}$$

Equation (6.6) is the adiabatic vaporization condition, and (6.7) and (6.8) state that the reservoir remains pure fuel. The ratio of heat of vaporization to heat of combustion is denoted by $\bar{L}$.

Whenever numerical results are sought, parameter values appropriate to the burning of acetone in air are used:

$$(\mathrm{CH_3})_2\mathrm{CO}+4\mathrm{O_2}\to 3(\mathrm{H_2O}+\mathrm{CO_2})$$

$d=1,\quad m=186,\quad (\overline{Y}_{\mathrm{O}})_\infty=0{\cdot}3371,\quad \overline{T}_B=0{\cdot}0593,$

$b=4,\quad \alpha_{\mathrm{F}}=3{\cdot}207,\quad \bar{\theta}=2{\cdot}441,\quad \bar{L}=0{\cdot}0169,$

$p=3,\quad \alpha_{\mathrm{O}}=1{\cdot}453,\quad \overline{T}_\infty=0{\cdot}0700,\quad C_P=0{\cdot}4118\,\mathrm{B.Th.U./lb.\,^\circ R.}$

$\Delta h_C/\alpha_{\mathrm{F}}C_P=1{\cdot}002\times10^4\,^\circ\mathrm{R},\quad D=0{\cdot}0908\ \mathrm{in.^2/sec\ at\ 1800\,^\circ R},$

$\rho=6.416\,\mathrm{g/l},\quad \bar{B}=1{\cdot}08\times10^{12}\,\mathrm{l/mole\,sec.}$

Relatively few analytic studies of burning in unpremixed gases exist for finite rate-of-reaction kinetics. Zeldovitch (1951), Spalding (1954, 1961), and Spalding & Jain (1962) claim to have detected suggestions of extinction conditions in the general properties of Arrhenius kinetics. Agafanova, Gurevich & Paliev (1958) tried to find extinction conditions by numerical integration for a fuel drop in an oxidant atmosphere but the results were indecisive. Lorell, Wise & Carr (1956) attempted the same solution and interpreted non-existence of solutions as $\bar{\theta}$ increased as proof of extinction. This statement implies some reactions are always extinguished, others never. Furthermore, their assertions that $\bar{\theta}\to 0$ carries second-order Arrhenius kinetics to Burke–Schumann kinetics is incorrect; $D_1\to\infty$ will be shown to effect the transition. Marble & Adamson (1954) used series-expansion techniques for a laminar mixing zone and Dooley (1956) similarity theory for a flat plate; both these works establish conditions under which reaction enters a balance of diffusion and convection, and ignition occurs.

In several papers of the later 1950's boundary-layer-like regions of sharp transition in basically smooth equilibrium profiles were recognized from numerical treatments of high rate-of-reaction limits. Lenard (1962) seems to have been the first to apply the schematics of inner and outer expansions in treating a chemically reacting flow in the limit of large first Damkohler number. Lenard discussed rapid relaxation to chemical equilibrium behind a shock. Linan (1963), arguing by physical intuition, has treated the laminar mixing zone in the large D_1 limit and found qualitative features in Arrhenius-kinetics solutions that hint at extinction conditions. Chin (1962) was the first to obtain the

Burke–Schumann solution for stagnation-region burning in initially unmixed reactants but his claims of finding exact extinction criteria for finite-rate kinetics are spurious. A correct formulation along the same lines as Chin's was carried out by Chambre (1956) to find the no-heat-transfer conditions in a premixed two-dimensional viscous stagnation-like flow toward an impermeable wall.

7. Thin-flame solution

The solution under Burke–Schumann kinetics is now presented. According to (6.3)

$$\overline{Y}_{\mathrm{O}}(\bar{z}) = \begin{cases} A_1 \operatorname{erf}(\bar{z}/\sqrt{2}) + B_1 & (\bar{z}_* < \bar{z} < \infty), \\ A_2 \operatorname{erf}(\bar{z}/\sqrt{2}) + B_2 & (\bar{z}_w < \bar{z} < \bar{z}_*). \end{cases}$$

Similar functional forms holds for $\overline{Y}_{\mathrm{F}}$ and $\overline{T}$. If equations (6.4)–(6.8), (5.2), and (5.3) are used to identify the constants of integration, $\bar{z}_w$, z_*, and $\overline{T}_*$, there results

$$\overline{Y}_{\mathrm{O}}(\bar{z}) = \begin{cases} \{(\overline{Y}_{\mathrm{O}})_\infty / \operatorname{erfc}(\bar{z}_*/\sqrt{2})\}\{\operatorname{erf}(\bar{z}/\sqrt{2}) - \operatorname{erf}(\bar{z}_*/\sqrt{2})\} & (\bar{z}_* \leqslant \bar{z} \leqslant \infty), \\ 0 & (\bar{z}_w \leqslant \bar{z} \leqslant \bar{z}_*); \end{cases}$$

$$\overline{Y}_{\mathrm{F}}(\bar{z}) = \begin{cases} 0 & (\bar{z}_* \leqslant \bar{z} \leqslant \infty), \\ (\overline{Y}_{\mathrm{F}})_w \{\operatorname{erf}(\bar{z}/\sqrt{2}) - \operatorname{erf}(\bar{z}_*/\sqrt{2})\}/\{\operatorname{erf}(\bar{z}_w/\sqrt{2}) - \operatorname{erf}(\bar{z}_*/\sqrt{2})\} & (\bar{z}_w \leqslant \bar{z} \leqslant \bar{z}_*); \end{cases}$$

$$\overline{T}(\bar{z}) = \begin{cases} \overline{T}_\infty + \dfrac{(\overline{T}_* - \overline{T}_\infty)\operatorname{erfc}(\bar{z}/\sqrt{2})}{\operatorname{erfc}(\bar{z}_*/\sqrt{2})} & (\bar{z}_* \leqslant \bar{z} \leqslant \infty); \\ \dfrac{(\overline{T}_* - \overline{T}_B)\{\operatorname{erf}(\bar{z}/\sqrt{2}) - \operatorname{erf}(\bar{z}_w/\sqrt{2})\}}{\{\operatorname{erf}(\bar{z}_*\sqrt{2}) - \operatorname{erf}(\bar{z}_w/\sqrt{2})\}} + \overline{T}_B & (\bar{z}_w \leqslant \bar{z} < \bar{z}_*); \end{cases}$$

$$\bar{z}_w = -\sqrt{\frac{2}{\pi}} \frac{(\overline{Y}_{\mathrm{O}})_\infty + (\overline{Y}_{\mathrm{F}})_w}{\alpha_{\mathrm{F}} - (\overline{Y}_{\mathrm{F}})_w} \frac{\exp(-\frac{1}{2}\bar{z}_w^2)}{\operatorname{erfc}(\bar{z}_w/\sqrt{2})}; \tag{7.1}$$

$$\overline{T}_* = \frac{(\overline{Y}_{\mathrm{O}})_\infty (\overline{Y}_{\mathrm{F}})_w}{(\overline{Y}_{\mathrm{O}})_\infty + (\overline{Y}_{\mathrm{F}})_w} + \frac{(\overline{Y}_{\mathrm{F}})_w \overline{T}_\infty + (\overline{Y}_{\mathrm{O}})_\infty \overline{T}_B}{(\overline{Y}_{\mathrm{O}})_\infty + (\overline{Y}_{\mathrm{F}})_w}; \tag{7.2}$$

$$(\overline{Y}_{\mathrm{F}})_w = \frac{\alpha_{\mathrm{F}}[\overline{T}_\infty + (\overline{Y}_{\mathrm{O}})_\infty - \bar{L}(\overline{Y}_{\mathrm{O}})_\infty - \overline{T}_B]}{(\overline{Y}_{\mathrm{O}})_\infty + \overline{T}_\infty - \overline{T}_B + \alpha_{\mathrm{F}}\bar{L}}; \tag{7.3}$$

$$\operatorname{erfc}(\bar{z}_*/\sqrt{2})/\operatorname{erfc}(\bar{z}_w/\sqrt{2}) = (\overline{Y}_{\mathrm{O}})_\infty / \{(\overline{Y}_{\mathrm{O}})_\infty + (\overline{Y}_{\mathrm{F}})_w\}. \tag{7.4}$$

The apparent flame strength is defined as

$$|d\overline{Y}_{\mathrm{F}}(\bar{z}_{*-})/d\bar{z}| = \{(\overline{Y}_{\mathrm{O}})_\infty + (\overline{Y}_{\mathrm{F}})_w\}(2/\pi)^{\frac{1}{2}} \exp(-\tfrac{1}{2}\bar{z}_*^2)/\operatorname{erfc}(\bar{z}_w/\sqrt{2}).$$

The flame temperature $\overline{T}_*$ is identical with the adiabatic flame temperature, the final temperature reached above the initial temperature when the fuel and oxidant species are premixed in stoichiometric proportion and then burned adiabatically and isobarically until an equilibrium mixture of reactants and products is attained. If $\overline{T}_* > \max[\overline{T}_\infty, \overline{T}(\bar{z}_w)]$, then $\overline{T}$ never exceeds $\overline{T}_*$ for any $\bar{z}$ for any D_1.

A numerical example of these formulae using the data given in § 6 appears as figure 2.

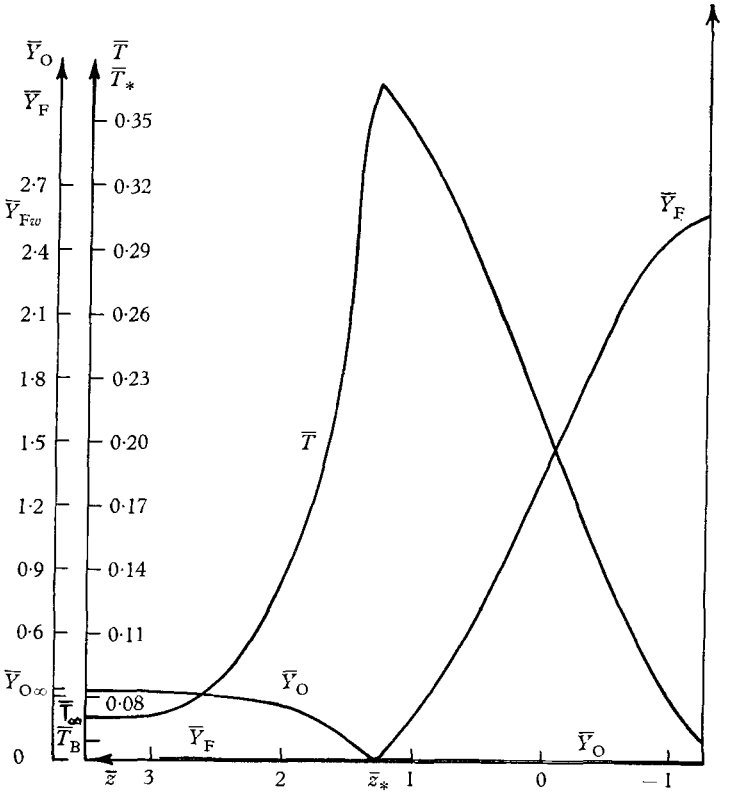

FIGURE 2. Thermal and mass concentration profiles for thin-flame kinetics. Input: $\overline{Y}_{O\infty} = 0{\cdot}3371$; $\overline{T}_\infty = 0{\cdot}0700$; $\overline{T}_B = 0{\cdot}0593$; $\alpha_F = 3{\cdot}207$; $\overline{L} = 0{\cdot}0169$. Output: $\bar{z}_w = -1{\cdot}2710$; $\overline{Y}_{Fw} = 2{\cdot}7292$; $\bar{z}_* = 1{\cdot}2888$; $\overline{T}_* = 0{\cdot}3689$; $|d\overline{Y}_F/d\bar{z}|_{\bar{z}_*} = 0{\cdot}5936$.

8. Nearly chemically frozen flow

An analytic solution in the asymptotic limit of small chemical activity is obtained for equations (6.1) subject to (6.4)–(6.8) by conventional perturbation expansion in a small parameter. To lowest order, diffusion balances convection, and reaction enters as a forcing function in the first-order solution. The solution is valid only for very small values of the expansion parameter $\epsilon = D_1 \exp(-\overline{\theta}/\overline{T}_\infty)$.

For small ϵ a solution to equations (6.1) subject to (6.4)–(6.8) is sought in the form

$$\begin{Bmatrix} \overline{Y}_O(\bar{z},\epsilon) \\ \overline{Y}_F(\bar{z},\epsilon) \\ \overline{T}(\bar{z},\epsilon) \\ \bar{z}_w(\epsilon) \end{Bmatrix} = \sum_{n=0} \epsilon^n \begin{Bmatrix} [\overline{Y}_O(\bar{z})]_n \\ [\overline{Y}_F(\bar{z})]_n \\ [\overline{T}(\bar{z})]_n \\ [\bar{z}_w]_n \end{Bmatrix}. \tag{8.1}$$

Substitution of (8.1) into (6.1) yields

$$L \begin{Bmatrix} [\overline{Y}_O(\bar{z})]_0 \\ [\overline{Y}_F(\bar{z})]_0 \\ [\overline{T}(\bar{z})]_0 \end{Bmatrix} = 0, \quad L = \frac{d}{d\bar{z}} \left(\exp(\tfrac{1}{2}\bar{z}^2) \frac{d}{d\bar{z}} \right), \tag{8.2}$$

$$L\begin{Bmatrix}\overline{Y}_{On}\\ \overline{Y}_{Fn}\\ \overline{T}_n\end{Bmatrix} = f_n \exp\left(-\frac{\overline{\theta}}{\overline{T}_0}+\frac{\overline{\theta}}{\overline{T}_\infty}+\frac{\bar{z}^2}{2}\right)\begin{Bmatrix}+1\\ +1\\ -1\end{Bmatrix}, \tag{8.3}$$

where

$$f_1 = \overline{Y}_{O0}\overline{Y}_{F0}, \quad f_2 = (\overline{T}_1\overline{\theta}/\overline{T}_0^2)\overline{Y}_{O0}\overline{Y}_{F0}+\overline{Y}_{F0}\overline{Y}_{O1}+\overline{Y}_{F1}\overline{Y}_{O0},$$

$$f_3 = \overline{Y}_{O0}\overline{Y}_{F0}(\overline{T}_1^2\overline{\theta}^2/2\overline{T}_0^4+\overline{T}_2\overline{\theta}/\overline{T}_0^2)+(\overline{T}_1\overline{\theta}/\overline{T}_0^2)(\overline{Y}_{F0}\overline{Y}_{O1}+\overline{Y}_{F1}\overline{Y}_{O0})$$
$$+\overline{Y}_{O2}\overline{Y}_{F0}+\overline{Y}_{F2}\overline{Y}_{O0}+\overline{Y}_{F1}\overline{Y}_{O1}, \text{ etc.}$$

Only the equations for the zero-order and first-order corrections will be treated here, though the methods could be continued to any order. The boundary conditions at infinity are:

$$\overline{T}_0(\infty) = \overline{T}_\infty, \quad \overline{Y}_{F0}(\infty) = 0, \quad \overline{Y}_{O0}(\infty) = (\overline{Y}_O)_\infty, \tag{8.4}$$

$$\overline{T}_n(\infty) = \overline{Y}_{Fn}(\infty) = \overline{Y}_{On}(\infty) = 0, \quad \text{for} \quad n > 0. \tag{8.5}$$

The zero-order boundary conditions at the two-phase interface are

$$\overline{T}_0(\bar{z}_{w0}) = \overline{T}_B, \tag{8.6}$$

$$d\overline{T}_0(\bar{z}_{w0})/d\bar{z} = -\alpha_F \bar{L}\bar{z}_{w0}, \tag{8.7}$$

$$\bar{z}_{w0}\overline{Y}_{O0}(\bar{z}_{w0}) + d\overline{Y}_{O0}(\bar{z}_{w0})/d\bar{z} = 0, \tag{8.8}$$

$$\bar{z}_{w0}[\alpha_F - \overline{Y}_{F0}(\bar{z}_{w0})] = d\overline{Y}_{F0}(\bar{z}_{w0})/d\bar{z}. \tag{8.9}$$

The solution of (8.2) subject to (8.4) and (8.6)–(8.9) is

$$\overline{Y}_{F0} = -\frac{\alpha_F \bar{z}_{w0}\operatorname{erfc}(\bar{z}/\sqrt{2})}{(2/\pi)^{\frac{1}{2}}\exp(-\frac{1}{2}\bar{z}_{w0}^2)-\bar{z}_{w0}\operatorname{erfc}(\bar{z}_{w0}/\sqrt{2})}, \tag{8.10}$$

$$\overline{Y}_{O0} = \frac{\overline{Y}_{O\infty}\bar{z}_{w0}\operatorname{erfc}(\bar{z}/\sqrt{2})}{(2/\pi)^{\frac{1}{2}}\exp(-\frac{1}{2}\bar{z}_{w0}^2)-\bar{z}_{w0}\operatorname{erfc}(\bar{z}_{w0}/\sqrt{2})}+\overline{Y}_{O\infty}, \tag{8.11}$$

$$\overline{T}_0 = \frac{(\overline{T}_B-\overline{T}_\infty)\operatorname{erfc}(\bar{z}/\sqrt{2})}{\operatorname{erfc}(\bar{z}_{w0}/\sqrt{2})}+\overline{T}_\infty, \tag{8.12}$$

$$\bar{z}_{w0} = \frac{(2/\pi)^{\frac{1}{2}}(\overline{T}_B-\overline{T}_\infty)\exp(-\frac{1}{2}\bar{z}_{w0}^2)}{\alpha_F \bar{L}\operatorname{erfc}(\bar{z}_{w0}/\sqrt{2})}. \tag{8.13}$$

Since $\bar{z}_w < 0$ is anticipated, equation (8.13) suggests $\overline{T}_\infty > \overline{T}_B$. If a steady-state solution with $\overline{T}(\bar{z}_w) = \overline{T}_B$ is demanded, the oxidant supply being blown at the wall must be relatively hot to continue vaporization because no heat of combustion is available to continue the vaporization in this frozen limit. The physically more suitable boundary condition, the Clausius–Clapeyron equation, would yield a wall temperature about 15 % lower than the boiling temperature for the acetone–air data given in § 6, for the near-frozen condition described here. For cases in which significant reaction occurs, $\overline{T}(\bar{z}_w) \to \overline{T}_B$ and the error is appreciably less. For $\overline{T}_\infty > \overline{T}_B$, equation (8.12) gives $\overline{T}_{\max}$ at infinity.

Insertion of the z_w expansion in (6.4)–(6.8) yields the first-order boundary conditions at the wall:

$$\bar{T}_1(\bar{z}_{w0}) = -\bar{z}_{w1}\,d\bar{T}_0(\bar{z}_{w0})/d\bar{z} = \bar{z}_{w1}(\bar{T}_B - \bar{T}_\infty)\,(2/\pi)^{\frac{1}{2}} \exp(-\tfrac{1}{2}\bar{z}_{w0}^2)/\operatorname{erfc}(\bar{z}_{w0}/\sqrt{2}), \tag{8.14}$$

$$\bar{z}_{w1} = -\frac{d\bar{T}_1(\bar{z}_{w0})/d\bar{z}}{\alpha_F \bar{L} + d^2\bar{T}_0(\bar{z}_{w0})/d\bar{z}^2} = \frac{-d\bar{T}_1(\bar{z}_{w0})/d\bar{z}}{\alpha_F \bar{L} + \bar{z}_{w0}(\bar{T}_B - \bar{T}_\infty)\,(2/\pi)^{\frac{1}{2}} \exp(-\tfrac{1}{2}\bar{z}_{w0}^2)/\operatorname{erfc}(\bar{z}_{w0}/\sqrt{2})}, \tag{8.15}$$

$$d\bar{Y}_{F1}(\bar{z}_{w0})/d\bar{z} = -\bar{z}_{w0}\bar{Y}_{F1}(\bar{z}_{w0}) - \bar{z}_{w1}\alpha_F\left\{1 + \frac{\bar{z}_{w0}\operatorname{erfc}(\bar{z}_{w0}/\sqrt{2})}{(2/\pi)^{\frac{1}{2}}\exp(\frac{1}{2}\bar{z}_{w0}^2) - \bar{z}_{w0}\operatorname{erfc}(\bar{z}_{w0}/\sqrt{2})}\right\}, \tag{8.16}$$

$$d\bar{Y}_{O1}(\bar{z}_{w0})/d\bar{z} = -\bar{z}_{w0}\bar{Y}_{O1}(\bar{z}_{w0}) - \bar{z}_{w1}\bar{Y}_{O\infty}\left\{1 + \frac{\bar{z}_{w0}\operatorname{erfc}(\bar{z}_{w0}/\sqrt{2})}{(2/\pi)^{\frac{1}{2}}\exp(\frac{1}{2}\bar{z}_{w0}^2) - \bar{z}_{w0}\operatorname{erfc}(\bar{z}_{w0}/\sqrt{2})}\right\}. \tag{8.17}$$

Solution of the equation for $\bar{T}_1$ of (8.3) subject to $\bar{T}_1(\infty) = 0$, (8.14) and (8.15) requires direct integration and an integration by parts or else a simple application of Green's function theory to obtain

$$\bar{T}_1(\bar{z}) = \frac{1}{(2/\pi)^{\frac{1}{2}}\operatorname{erfc}(\bar{z}_{w0}/\sqrt{2})}\left\{\operatorname{erfc}(\bar{z}/\sqrt{2})\int_{\bar{z}_{w0}}^{\infty} g_1(\xi)\{\operatorname{erf}(\xi/\sqrt{2}) - \operatorname{erf}(\bar{z}_{w0}/\sqrt{2})\}\,d\xi + \{\operatorname{erf}(\bar{z}/\sqrt{2}) - \operatorname{erf}(\bar{z}_{w0}/\sqrt{2})\}\int_{\bar{z}}^{\infty} g_1(\xi)\operatorname{erfc}(\xi/\sqrt{2})\,d\xi\right\} - \operatorname{erfc}(\bar{z}/\sqrt{2})\left\{\frac{\bar{z}_{w1}\exp(-\tfrac{1}{2}\bar{z}_{w0}^2)\,(2/\pi)^{\frac{1}{2}}(\bar{T}_\infty - \bar{T}_B)}{[\operatorname{erfc}(\bar{z}_{w0}/\sqrt{2})]^2}\right\}, \tag{8.18}$$

where $g_1(\xi) = \bar{Y}_{O0}(\xi)\,\bar{Y}_{F0}(\xi)\exp\{-\bar{\theta}/\bar{T}_0(\xi) + \bar{\theta}/\bar{T}_\infty + \frac{1}{2}\xi^2\}$. By Leibnitz's rule

$$\bar{z}_{w1} = -\frac{\exp(-\tfrac{1}{2}\bar{z}_{w0}^2)\int_{\bar{z}_{w0}}^{\infty} g_1(\xi)\operatorname{erfc}(\xi/\sqrt{2})\,d\xi}{\alpha_F\bar{L}\operatorname{erfc}(\bar{z}_{w0}/\sqrt{2}) - (2/\pi)^{\frac{1}{2}}\bar{z}_{w0}\exp(-\bar{z}_{w0}^2/2)\,(\bar{T}_\infty - \bar{T}_B) + (2/\pi)\exp(-\bar{z}_{w0}^2)\,(\bar{T}_\infty - \bar{T}_B)/\operatorname{erfc}(\bar{z}_{w0}/\sqrt{2})}. \tag{8.19}$$

$\bar{T}_1$ is seen to be positive definite so burning augments the temperature for $\bar{z}_w < \bar{z} < \infty$. If $\bar{T}_0(\bar{z})$ were a peaked function, steepest-descent evaluation would be suitable but in the present case numerical integration is required. Very roughly the inequality $\epsilon\bar{\theta}\bar{T}_1/\bar{T}_0^2 \ll 1$ used in obtaining successive f_n can be written as $D_1 \ll \bar{T}_\infty/\bar{\theta})\exp(\bar{\theta}/\bar{T}_\infty)\,\bar{L}$ (const.). The series fails for smaller D_1 if $\bar{L} \ll 1$, where $\bar{L}$ is the ratio of heat of vaporization to heat of combustion. Thus the series would fail sooner for octane than for acetone.

The numerical results for small rates of reaction for acetone–air combustion will be presented below after the formalism for other rates of reaction is developed.

9. Nearly thin-flame conditions

For very large but finite D_1 (typical chemistry time very short relative to flow time) a narrow region of intense burning near $\bar{z}_*$ can be described by the inner and outer expansions of a singular perturbation. The maximum temperatures realized should be just slightly smaller than the adiabatic flame temperature. At positions removed from the immediate vicinity of the steep gradients of the flame, the conditions for D_1 large should be approximately those for infinite D_1 (the Burke–Schumann solution).

A three-part solution is presented:

(1) an upstream outer region (between infinity and the flame) where oxidant is preheated and fuel is not found;

(2) an inner region near $\bar{z}_*$ in which an intense flame occurs and conduction and diffusion are the dominant modes of transport; and

(3) a downstream outer region (between the flame and the wall) where fuel is preheated and oxidant is not found.

If $\epsilon = D_1^{-1}$, for $\epsilon = 0$, $\overline{Y}_O \overline{Y}_F = 0$ everywhere. For the case of interest here, $\epsilon \ll 1$, $\overline{Y}_O \overline{Y}_F = 0$ except where the steepness of derivatives overcomes the smallness of the multiplicative parameter. In the anticipation that convection and diffusion dominate the outer expansions and molecular transports and chemical activity the inner expansion, solution of (6.1) subject to (6.4)–(6.8) is sought in the form

(1) upstream outer expansion:

$$\overline{T}_u(\bar{z},\epsilon) = \overline{T}_u(\bar{z}), \quad \overline{Y}_{Ou}(\bar{z},\epsilon) = \overline{Y}_{Ou}(\bar{z}), \quad \overline{Y}_{Fu}(\bar{z},\epsilon) = 0;$$

(2) inner expansion:

$$\begin{aligned}
\overline{Y}_{Oi}(\bar{z},\epsilon) &= \epsilon^{\frac{1}{3}}\overline{y}_{O1}(\eta) + \epsilon^{\frac{2}{3}}\overline{y}_{O2}(\eta) + \ldots, \\
\overline{Y}_{Fi}(\bar{z},\epsilon) &= \epsilon^{\frac{1}{3}}\overline{y}_{F1}(\eta) + \epsilon^{\frac{2}{3}}\overline{y}_{F2}(\eta) + \ldots, \\
\overline{T}_i(\bar{z},\epsilon) - \overline{T}_* &= \epsilon^{\frac{1}{3}}\bar{t}_1(\eta) + \epsilon^{\frac{2}{3}}\bar{t}_2(\eta) + \ldots;
\end{aligned}$$

(3) downstream outer expansion:

$$\overline{T}_d(\bar{z},\epsilon) = \overline{T}_d(\bar{z}), \quad \overline{Y}_{Fd}(\bar{z},\epsilon) = \overline{Y}_{Fd}(\bar{z}), \quad \overline{Y}_{Od}(\bar{z},\epsilon) = 0;$$

where $\eta = (\bar{z} - \bar{z}_*)/\epsilon^{\frac{1}{3}}$. The lowest-order outer term will match more and more exactly as successive terms are added to the inner expansion. As a result the higher-order outer terms will be described by homogeneous equations subject to homogeneous boundary conditions, and thus vanish identically.

Substitution of the outer expressions into the equations (6.1) for finite ϵ yields, upon use of the boundary conditions (6.4)–(6.8):

$$\overline{Y}_{Ou} = -\overline{T}_u - A\,\mathrm{erfc}\,(\bar{z}/\sqrt{2}) + \overline{Y}_{O\infty} + \overline{T}_\infty, \tag{9.1}$$

$$\overline{T}_u = -C\,\mathrm{erfc}\,(\bar{z}/\sqrt{2}) + \overline{T}_\infty, \tag{9.2}$$

$$\overline{Y}_{Fd} = -\overline{T}_d + D\{\mathrm{erf}\,(\bar{z}/\sqrt{2}) - \mathrm{erf}\,(\bar{z}_w/\sqrt{2})\} + \overline{Y}_{Fw} + \overline{T}_B, \tag{9.3}$$

$$\overline{T}_d = E\{\mathrm{erf}\,(\bar{z}/\sqrt{2}) - \mathrm{erf}\,(\bar{z}_w/\sqrt{2})\} + \overline{T}_B, \tag{9.4}$$

$$\bar{z}_w = (D-E)\,(2/\pi)^{\frac{1}{2}} \exp\,(-\tfrac{1}{2}\bar{z}_w^2)/(\alpha_F - \overline{Y}_{Fw}), \tag{9.5}$$

$$\overline{Y}_{Fw} = \alpha_F\{1 + \bar{L}(D-E)/E\}, \tag{9.6}$$

where A, C, D and E will be found by merging with the inner expansion. These outer solutions have the familiar error function form arising from diffusion-convection balance, and will be shown to be identical with the thin-flame solutions.

To lowest order the inner equations are

$$d^2\bar{y}_{O1}/d\eta^2 = \bar{y}_{O1}\bar{y}_{F1}\exp(-\bar{\theta}/\bar{T}_*) + O(\epsilon^{\frac{1}{3}}),$$
$$d^2\bar{y}_{F1}/d\eta^2 = \bar{y}_{O1}\bar{y}_{F1}\exp(-\bar{\theta}/\bar{T}_*) + O(\epsilon^{\frac{1}{3}}),$$
$$d^2\bar{t}_1/d\eta^2 = -\bar{y}_{O1}\bar{y}_{F1}\exp(-\bar{\theta}/\bar{T}_*) + O(\epsilon^{\frac{1}{3}}).$$

Schvab–Zeldovitch integrals again reduce this coupled sixth-order set to a second-order equation for one unknown:

$$\bar{y}_{O1} + \bar{t}_1 = \alpha\eta + \beta\epsilon^{-\frac{1}{3}}, \tag{9.7}$$

$$\bar{y}_{F1} + \bar{t}_1 = \gamma\eta + \delta\epsilon^{-\frac{1}{3}}, \tag{9.8}$$

$$d^2\bar{t}_1/d\eta^2 = -(\alpha\eta + \beta\epsilon^{-\frac{1}{3}} - \bar{t}_1)(\gamma\eta + \delta\epsilon^{-\frac{1}{3}} - \bar{t}_1)\exp(-\bar{\theta}/\bar{T}_*), \tag{9.9}$$

where

$$\bar{t}_1 \to \alpha\eta + \beta\epsilon^{-\frac{1}{3}} \quad \text{as} \quad \eta \to -\infty \quad (\text{so } \bar{y}_{O1} \to 0), \tag{9.10}$$

$$\bar{t}_1 \to \gamma\eta + \delta\epsilon^{-\frac{1}{3}} \quad \text{as} \quad \eta \to +\infty \quad (\text{so } \bar{y}_{F1} \to 0). \tag{9.11}$$

Writing the constants with ϵ factors is done merely for convenience.

Before the inner solution to lowest order is completed, matching of the inner and outer solutions is carried out in terms of an intermediate limit. If

$$\bar{z} - \bar{z}_* = \bar{z}_\xi\,\xi(\epsilon) \quad \text{where} \quad 0 < \epsilon^{\frac{1}{3}} < \xi(\epsilon) \quad \text{as} \quad \epsilon \to 0,$$

then

$$\lim_{\epsilon \to 0,\ \bar{z}_\xi \text{ fixed}} (\bar{z} - \bar{z}_*) = \bar{z}_\xi\,\xi(\epsilon) \to 0$$

but

$$\lim_{\epsilon \to 0,\ \bar{z}_\xi \text{ fixed}} \eta = \frac{\bar{z} - \bar{z}_*}{\epsilon^{\frac{1}{3}}} = \frac{\bar{z}_\xi\,\xi(\epsilon)}{\epsilon^{\frac{1}{3}}} \to \pm\infty.$$

Equations (9.1)–(9.4) are expressed in terms of $\bar{z}_\xi$:

$$\bar{Y}_{Ou} + \bar{T}_u = -A\,\mathrm{erfc}(\bar{z}_*/\sqrt{2}) + \bar{Y}_{O\infty} + \bar{T}_\infty + A(2/\pi)^{\frac{1}{2}}\exp(-\tfrac{1}{2}\bar{z}_*^2)\,\bar{z}_\xi\,\xi(\epsilon) + \ldots, \tag{9.12}$$

$$\bar{Y}_{Fd} + \bar{T}_d = D\{\mathrm{erf}(\bar{z}_*/\sqrt{2}) - \mathrm{erf}(\bar{z}_w/\sqrt{2})\} + \bar{T}_B + \bar{Y}_{Fw} + D(2/\pi)^{\frac{1}{2}}\exp(-\tfrac{1}{2}\bar{z}_*^2)\,\bar{z}_\xi\,\xi(\epsilon) + \ldots, \tag{9.13}$$

$$\bar{T}_u = -C\,\mathrm{erfc}(\bar{z}_*/\sqrt{2}) + \bar{T}_\infty + (2/\pi)^{\frac{1}{2}}\exp(-\tfrac{1}{2}\bar{z}_*^2)\,\bar{z}_\xi\,\xi(\epsilon) + \ldots, \tag{9.14}$$

$$\bar{T}_d = E\{\mathrm{erf}(\bar{z}_*/\sqrt{2}) - \mathrm{erf}(\bar{z}_w/\sqrt{2})\} + \bar{T}_B + E(2/\pi)^{\frac{1}{2}}\exp(-\tfrac{1}{2}\bar{z}_*^2)\,\bar{z}_\xi\,\xi(\epsilon) + \ldots. \tag{9.15}$$

Equations (9.7), (9.8), (9.10) and (9.11) give

$$\bar{Y}_{Oi} + \bar{T}_i = \alpha\bar{z}_\xi\,\xi(\epsilon) + (\beta + \bar{T}_*) + \ldots, \tag{9.16}$$

$$\bar{T}_{Fi} + \bar{T}_i = \gamma\bar{z}_\xi\,\xi(\epsilon) + (\delta + \bar{T}_*) + \ldots, \tag{9.17}$$

$$\bar{T}_i \to \alpha\bar{z}_\xi\,\xi(\epsilon) + (\beta + \bar{T}_*) + \ldots \quad \text{as} \quad \eta \to -\infty, \tag{9.18}$$

$$\bar{T}_i \to \gamma\bar{z}_\xi\,\xi(\epsilon) + (\delta + \bar{T}_*) + \ldots \quad \text{as} \quad \eta \to +\infty. \tag{9.19}$$

Matching these last two sets to lowest order, it is necessary that

$$\alpha = A(2/\pi)^{\frac{1}{2}} \exp(-\tfrac{1}{2}\bar{z}_*^2), \tag{9.20}$$

$$\beta + \overline{T}_* = -A \operatorname{erfc}(\bar{z}_*/\sqrt{2}) + \overline{Y}_{O\infty} + \overline{T}_\infty, \tag{9.21}$$

$$\gamma = D(2/\pi)^{\frac{1}{2}} \exp(-\tfrac{1}{2}\bar{z}_*^2), \tag{9.22}$$

$$\delta + \overline{T}_* = D\{\operatorname{erf}(\bar{z}_*/\sqrt{2}) - \operatorname{erf}(\bar{z}_w/\sqrt{2})\} + \overline{Y}_{Fw} + \overline{T}_B. \tag{9.23}$$

Substituting from (9.20) and (9.21) in (9.18), and matching the result to (9.15) yields

$$A = E = (\overline{Y}_{O\infty} + \overline{T}_\infty - \overline{T}_B)/\operatorname{erfc}(\bar{z}_w/\sqrt{2}). \tag{9.24}$$

Substituting from (9.22) and (9.23) in (9.19), and matching the result to (9.14) yields

$$D = C(-\overline{Y}_{Fw} + \overline{T}_\infty - \overline{T}_B)/\operatorname{erfc}(\bar{z}_w/\sqrt{2}). \tag{9.25}$$

Equations (9.24) and (9.25) when substituted in (9.5) and (9.6) give

$$\overline{Y}_{Fw} = \alpha_F \left\{ \frac{\overline{T}_\infty - \overline{T}_B + \overline{Y}_{O\infty}(1-\bar{L})}{\overline{T}_\infty - \overline{T}_B + \alpha_F \bar{L} + \overline{Y}_{O\infty}} \right\}, \tag{9.26}$$

$$-\bar{z}_w = \sqrt{\frac{2}{\pi}} \frac{\exp(-\tfrac{1}{2}\bar{z}_w^2)}{\operatorname{erfc}(\bar{z}_w/\sqrt{2})} \left\{ \frac{\overline{Y}_{Fw} + \overline{Y}_{O\infty}}{\alpha_F - \overline{Y}_{Fw}} \right\}. \tag{9.27}$$

Inserting from (7.2), (7.4), and (9.24) in (9.21) gives $\beta = 0$. Inserting from (7.2), (7.4), and (9.25) in (9.23) gives $\delta = 0$. Use of the same relations makes it possible to manipulate (9.1)–(9.4) into the forms for $\overline{Y}_F$, $\overline{Y}_O$ and $\overline{T}$ given as the thin-flame solution in § 7.

Equations (9.9)–(9.11) are now simplified because $\beta = \delta = 0$. If

$$\Lambda = Q[-\bar{t}_1 + \tfrac{1}{2}(\alpha+\gamma)\eta], \tag{9.28}$$

$$\chi = \tfrac{1}{2}Q(\alpha-\gamma)\eta, \tag{9.29}$$

$$Q^3 = \exp(-\bar{\theta}/\overline{T}_*)/[\tfrac{1}{2}(\alpha-\gamma)]^2, \tag{9.30}$$

then (9.9)–(9.11) become

$$d^2\Lambda(\chi)/d\chi^2 = \Lambda^2 - \chi^2 \quad (-\infty \leqslant \chi \leqslant \infty),$$
$$\Lambda \to \chi \quad \text{as} \quad \chi \to \infty,$$
$$\Lambda \to -\chi \quad \text{as} \quad \chi \to -\infty.$$

This boundary problem was solved numerically and the solution is given as figure 3, in recognition of the fact that Λ is an even function of χ. An approximate closed expression for $\Lambda(\chi)$ is given in the Appendix.

The expression for the temperature in the inner region by (9.28)–(9.30) is

$$\overline{T}_i = \overline{T}_* + \tfrac{1}{2}(\alpha+\gamma)(\bar{z}-\bar{z}_*) - (\epsilon/\Omega)^{\frac{1}{3}} \Lambda\{(\Omega/\epsilon)^{\frac{1}{3}} \tfrac{1}{2}(\alpha-\gamma)(\bar{z}-\bar{z}_*)\}. \tag{9.31}$$

Using (9.31) to find $d\overline{T}_i/d\bar{z} = 0$, it is found that the maximum temperature occurs at χ_M, not in general $\bar{z} = \bar{z}_*$, where χ_M is given by

$$\frac{d\Lambda(\chi_M)}{d\chi} = \frac{\alpha+\gamma}{\alpha-\gamma} = \frac{A+D}{A-D} = \frac{\overline{Y}_{O\infty} - \overline{Y}_{Fw} + 2(\overline{T}_\infty - \overline{T}_B)}{\overline{Y}_{Fw} + \overline{Y}_{O\infty}}. \tag{9.32}$$

If $$\overline{T}_\infty \approx \overline{T}_B, \quad \overline{Y}_{O\infty} > \overline{Y}_{Fw} \Rightarrow d\Lambda(\chi_M)/d\chi > 0 \Rightarrow \chi_M > 0$$

$\Rightarrow$ maximum temperature occurs on the oxidant side of the thin flame. If $\overline{T}_\infty \approx \overline{T}_B$ but $\overline{Y}_{Fw} > \overline{Y}_O$, it follows similarly that the maximum temperature occurs on the fuel side. Only if $[2(\overline{T}_\infty - \overline{T}_B) + \overline{Y}_{O\infty} - \overline{Y}_{Fw}] = 0$ does the maximum temperature not become displaced from its thin-flame position $\bar{z}_*$. From (9.29)

$$\chi_M = \Omega^{\frac{1}{3}} \tfrac{1}{2}(\alpha - \gamma)(\bar{z}_M - \bar{z}_*)/\epsilon^{\frac{1}{3}}. \tag{9.33}$$

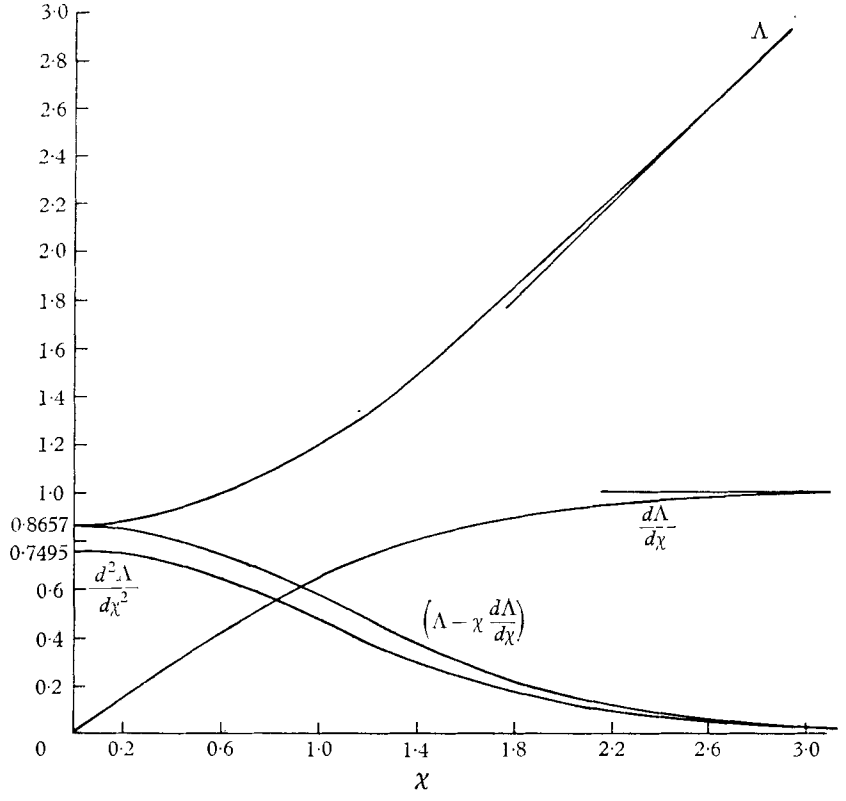

FIGURE 3. Plot of the solution of $d^2\Lambda/d\chi^2 = \Lambda^2 - \chi^2$ subject to $d\Lambda(\infty)/d\chi \to 1$ and $d\Lambda(0)/d\chi = 0$.

Inserting (9.32) and (9.33) in (9.31)

$$\overline{T}_i(\bar{z}_M) = \overline{T}_* - (\epsilon/\Omega)^{\frac{1}{3}} |\Lambda(\chi_M) - \chi_M d\Lambda(\chi_M)/d\chi| \tag{9.34}$$

to lowest order. For large but finite D_1, decrease of D_1 while all the other parameters are held fixed implies decrease of $\overline{T}_{\max}$.

To obtain the error in (9.34) one must proceed to the equations of first order governing the inner zone, found by substituting the inner expansion into (6.1) and retaining terms of $O(\epsilon^{\frac{2}{3}})$. This set (and all succeeding sets) of equations is linear; the homogeneous operator describes a reaction-diffusion balance and the inhomogeneous forcing function represents convection.

$$d^2\bar{y}_{O2}/d\eta^2 - \bar{y}_{F1}\bar{y}_{O2}\exp(-\bar{\theta}/\overline{T}_*) - \bar{y}_{O1}\bar{y}_{F2}\exp(-\bar{\theta}/\overline{T}_*) = -\bar{z}_* d\bar{y}_{O1}/d\eta, \tag{9.35}$$

$$d^2\bar{y}_{F2}/d\eta^2 - \bar{y}_{O1}\bar{y}_{F2}\exp(-\bar{\theta}/\overline{T}_* - \bar{y}_{F1}\bar{y}_{O2}\exp(-\bar{\theta}/\overline{T}_*) = -\bar{z}_* d\bar{y}_{F1}/d\eta, \tag{9.36}$$

$$d^2\bar{t}_2/d\eta^2 + \bar{y}_{O1}\bar{y}_{F2}\exp(-\bar{\theta}/\overline{T}_*) + \bar{y}_{F1}\bar{y}_{O2}\exp(-\bar{\theta}/\overline{T}_*) = -\bar{z}_* d\bar{t}_1/d\eta. \tag{9.37}$$

The terms with subscript unity are now known functions of η, although they are known exactly only in tabular form because Λ required numerical solution. The set has been only incompletely dealt with (Fendell 1964) but the adopted inner expansion has been justified and (9.34) can be written

$$\bar{T}(\bar{z}_M) = \bar{T}_* - (\epsilon/\Omega)^{\frac{1}{3}} |\Lambda(\chi_M) - \chi_M \, d\Lambda(\chi_M)/d\chi| + O(\epsilon^{\frac{2}{3}}). \tag{9.38}$$

Again, presentation of results for the acetone-in-air case is postponed until the intermediate range of reaction rates is examined.

10. Numerical integration

The asymptotic expansion for nearly frozen flow under second-order Arrhenius kinetics and the asymptotic expansion for nearly thin-flame conditions appear to both be valid for a range of intermediate D_1 but describe quite divergent profiles of the dependent variables *vs* $\bar{z}$. For continuous variation of behaviour with the parameter D_1 an intermediate branch is sought numerically (because of non-linearities) to join the upper branch (singular perturbation solution) and the lower branch (regular perturbation solution). Bifurcation of solution in steady-state stability analyses is familiar from several classical problems of continuum mechanics.

For solution on the IBM 7094 computer the non-linear two-point boundary-value problem of (6.1), (6.4)–(6.8) was written

$$d\bar{T}/d\bar{z} = \bar{v},$$

$$d\bar{v}/d\bar{z} = -\bar{z}\bar{v} - D_1 \exp(-\bar{\theta}/\bar{T}) \{-\bar{T} + \bar{Y}_{O\infty} + \bar{T}_\infty - A \operatorname{erfc}(\bar{z}/\sqrt{2})\} \{-\bar{T} + \bar{T}_\infty - C \operatorname{erfc}(\bar{z}/\sqrt{2})\},$$

where

$$A = F[\bar{Y}_{O\infty} + \bar{T}_\infty - \bar{T}_B + \alpha_F \bar{L}],$$

$$C = F[\bar{T}_\infty - \bar{T}_B - \alpha_F(1 - \bar{L})],$$

$$F = \bar{z}_w/[\bar{z}_w \operatorname{erfc}(\bar{z}_w/\sqrt{2}) - (2/\pi)^{\frac{1}{2}} \exp(-\tfrac{1}{2}\bar{z}_w^2)]$$

subject to

$$\bar{T}(\infty) = \bar{T}_\infty, \quad \bar{T}(\bar{z}_w) = \bar{T}_B, \quad \bar{v}(\bar{z}_w) = -\alpha_F \bar{L} \bar{z}_w.$$

A sequence of initial-value problems were solved by adopting values for $\bar{z}_w$ until a pair leading to values of $\bar{T}$ at infinity bounding the value $\bar{T}_\infty$ were found—infinity being considered reached upon suitably constant behaviour of $\bar{T}$ and its first derivative. Once bounding $\bar{z}_w$ were established linear interpolation in the form of a false-position method was used to converge on the correct $\bar{z}_w$. The integration technique was Runge's version of the fourth-order Runge–Kutta method, as improved by Richardson's extrapolation procedure.

While solutions for moderate or little burning intensity were readily found, the step-size had to be reduced to time-consuming minuteness and the initial conditions established precisely for intense-burning solutions. Basically, low-order polynomial approximation had difficulty treating the rapidly varying behaviour of dependent variables in the boundary-layer regions.

The results of the numerical integration for the acetone–air data are seen most directly from figure 4, in which the maximum temperature is plotted against D_1, with the analytically computed curves of §§ 7 and 8 sketched in. Two reverses in

curvature distinguish a lower (weak burning), middle (intermediate burning), and upper (intense burning) branch. Thus if the curve of figure 4 is traced from $D_1 = 0$ to $D_1 \to \infty$ a succession of steady states of constantly increased burning are passed. The wall position $\bar{z}_w$ is constantly receding to algebraically smaller $\bar{z}$, $\overline{Y}_O(\bar{z}_w)$ is constantly becoming smaller and $\overline{Y}_F(\bar{z}_w)$ larger. A more pronounced burning region may be distinguished through which $\overline{Y}_O$ and $\overline{Y}_F$ change rapidly in value, and $\overline{T}$ more clearly and sharply peaks. Illustration of these statements is provided in figures 5, 6, 7, and 8. Figure 8 shows that the position of maximum temperature does not vary monotonically, like the other quantities: $\bar{z}_M$ becomes smaller until just before the corner between the intermediate and upper branches

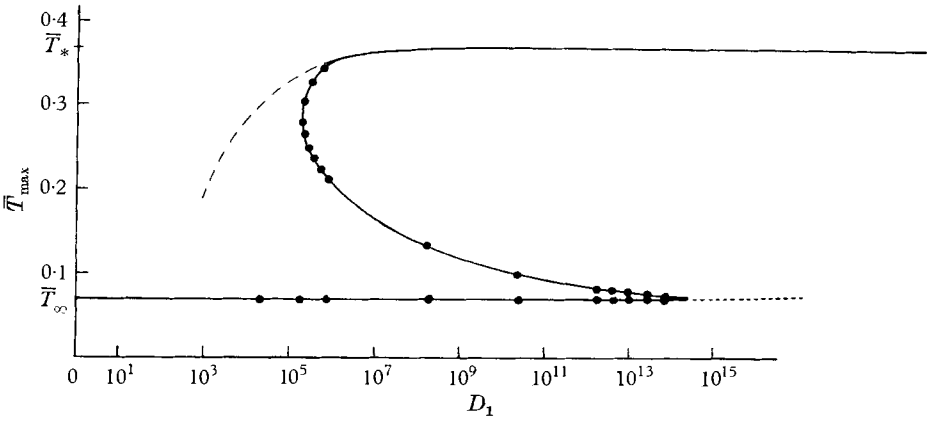

FIGURE 4. Plot of maximum temperature *vs* first Damkohler similarity group. The solid curve is based on numerical results and asymptotic analytic forms. The dotted line is the deviating regular-perturbation solution, and the dashed line the deviating singular-perturbation expansion. The points are the results of numerical computations.

of figure 4 is approached; from that corner out to $D_1 \to \infty$, $\bar{z}_M$ increases. Physically as the upper branch is approached the temperatures being realized are such that vaporization is not as important a consideration as establishing the flame near the 'stoichiometric-ratio position'. Maintaining that intense burning is occurring and yet permitting a significant concentration of oxidant near the wall is inconsistent, and the flame moves off.

One circumstance concerning the role of a in D_1 deserves further comment. Figure 8 implies that, as D_1 is increased in the vicinity of $D_1 = 5 \times 10^{13}$ for a system on the weak-burning branch, the system must spontaneously ignite. A means of increasing D_1 would be to decrease a, the strength of blowing of oxidant from upstream infinity. That mere reduction of the supply of convected oxidant should cause the system to burst into flames may seem to contradict one's physical intuition. Actually, however, an examination of the geometric scales resolves the difficulty. $D_1 = 5 \times 10^{13} \Rightarrow a \approx 5 \times 10^{-5}\,\mathrm{sec}^{-1}$ for acetone in air, and the wall is about 4·25 in. from the stagnation plane. The velocity of a fluid element near the wall is then 4×10^{-4} in./sec and the element would require $\frac{3}{4}$ h to move an inch. In fact, an oxidant particle would have to be 275 yd. upstream of the stagnation plane to move at 1 in./sec. Obviously a disturbance

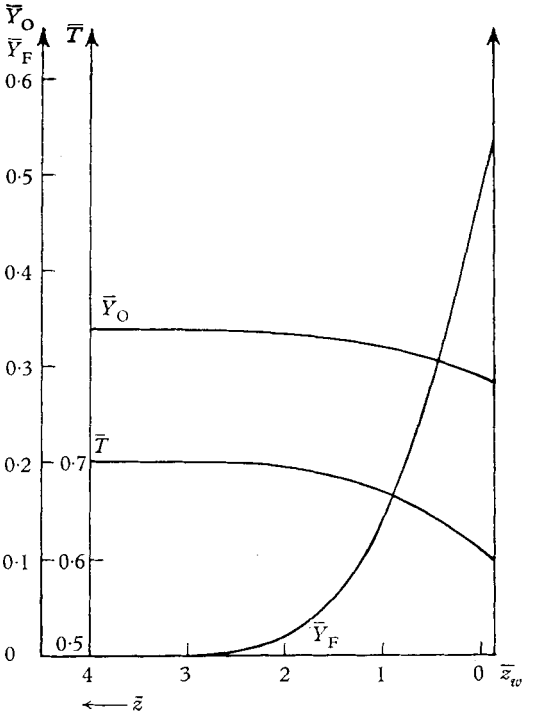

FIGURE 5. A typical solution from the low-burning branch. $D_1 = 10^8$; $\bar{z}_w = -0{\cdot}1402$; $\bar{Y}_{Fw} = 0{\cdot}5284$; $\bar{Y}_{Ow} = 0{\cdot}2816$; $(d\bar{T}/d\bar{z})_{max} = 7{\cdot}600 \times 10^{-3}$ at $\bar{z} = \bar{z}_w$.

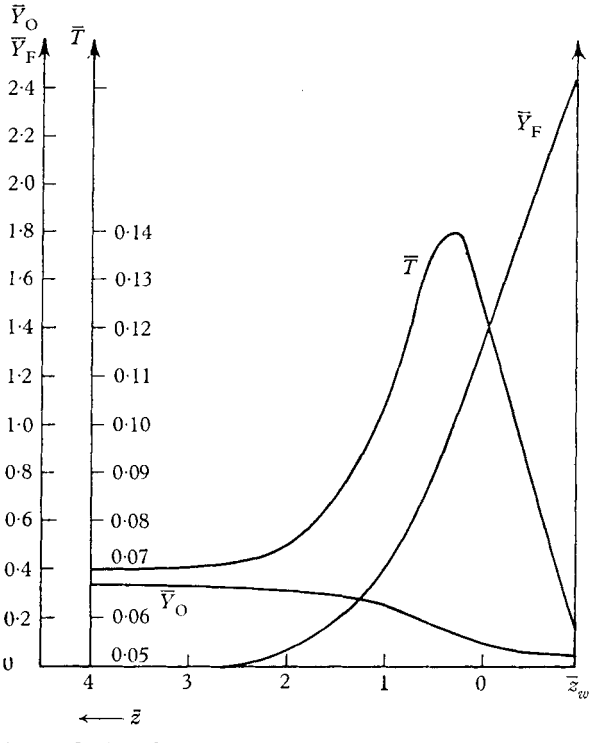

FIGURE 6. A typical solution from the intermediate branch. $D_1 = 10^8$; $\bar{z}_w = -0{\cdot}9434$; $\bar{Y}_{Fw} = 2{\cdot}3775$; $\bar{Y}_{Ow} = 4{\cdot}4989 \times 10^{-2}$; $(d\bar{T}/d\bar{z})_{max} \approx 6{\cdot}659 \times 10^{-2}$ at $\bar{z} \approx 0{\cdot}66$.

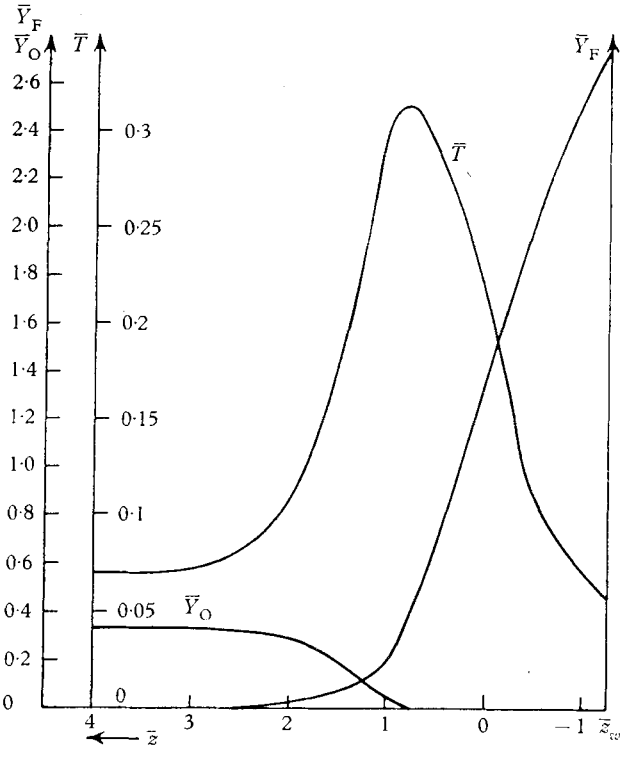

FIGURE 7. A typical solution from the intense-burning branch. $D_1 = 3{\cdot}5 \times 10^5$; $\bar{z}_w = -1{\cdot}2704$; $\bar{Y}_{Fw} = 2{\cdot}7287$; $(d\bar{T}/d\bar{z})_{\max} \approx 0{\cdot}2778$ at $\bar{z} \approx 1{\cdot}23$.

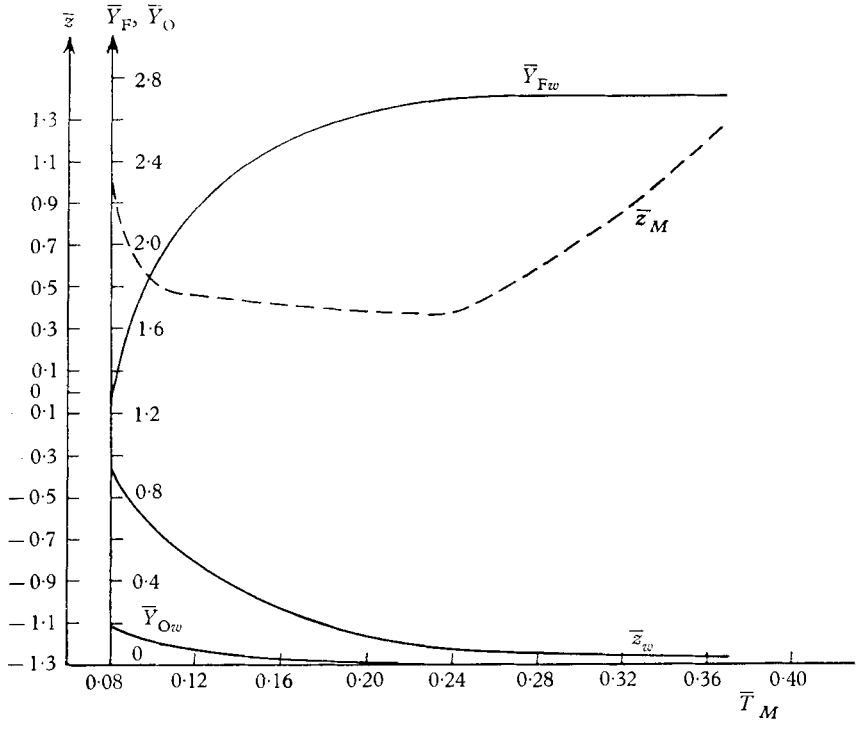

FIGURE 8. Plot of $\bar{z}_w$, $\bar{z}_m$, $\bar{Y}_{Fw}$ and $\bar{Y}_{Ow}$ *vs* $\bar{T}_M$. $\bar{T}_M$ = max. temperature; $\bar{z}_M$ = position of $\bar{T}_M$; $\bar{z}_w$ = position of two-phase interface; $\bar{Y}_{Ow}$ = oxidant concentration at $\bar{z}_w$; $\bar{Y}_{Fw}$ = fuel concentration at $\bar{z}_w$.

of even the slightest magnitude would upset the flow field completely. Furthermore, Arrhenius kinetics predicts a finite though small probability of reaction-inducing collision occurring even for temperatures of the order of 500–600 °R. Thus in the long time required for a particle to be convected through the region where oxidant and fuel are both plentiful, most reactants could quite reasonably pass to product. Considerable time would be required for the heat released in the exothermic reaction to be removed from the vicinity of the reaction in the large-scaled system being discussed. The temperatures would be locally increased, and this in turn would greatly raise the likelihood of reaction under Arrhenius kinetics. Thus sudden ignition under reduced blowing could reasonably occur in the system under analytic study, but such a system could only be realized under impossibly ideal laboratory conditions.

11. Conclusions

The problem of stagnation-region combustion of initially separated reactants has served as a means of examining the sufficiency of a simple model of the chemical kinetics to describe ignition and extinction. The role of the first Damkohler similarity group, the ratio of the time for a fluid particle of reactant to traverse the combustion zone to the time for a reaction-inducing collision to occur, has been clarified. For small D_1 there ought to be mainly diffusion and convection; for large D_1, vigorous spatially confined reaction. By use of the thermal profile as a guide for exothermic reactions this intuitive dependence has been confirmed. Finally Burke–Schumann kinetics has been shown (not assumed) to be the natural limit of Arrhenius kinetics as $D_1 \to \infty$.

Furthermore, unlike Burke–Schumann kinetics, Arrhenius kinetics has been shown to be able to describe ignition and extinction according to the following speculative interpretation of the bifurcated, three-branched steady-state solution presented in § 9. The middle branch is physically unstable and rarely observed; a system existing in such a condition will move toward the weak- or strong-burning branches, which are stable and normally observed. A system ignites when it jumps from the weak branch to the strong branch; suddenly, intense combustion instead of almost no combustion becomes the preferred state. This situation probably occurs as D_1 increases for a system on the lower branch. Analogously, as D_1 decreases for a system on the upper branch, it would have increasing propensity under sufficiently strong perturbation to cross over suddenly to the weak branch: this is extinction. Only a stability analysis with time development could suggest which transitions are possible or likely.

Appendix

An approximate closed form for Λ will now be developed by means of a crude application of certain techniques developed by Meksyn for second-order ordinary differential equations with rapidly decaying second derivative. Figure 3 suggests that Λ possesses this property. The presentation of the method will be such that techniques for improving the approximation will be apparent.

Meksyn proposes writing

$$d^2\Lambda/d\chi^2 = \Lambda^2 - \chi^2 = \exp[-F(\chi)]\,\phi(\chi),$$

where $\phi(\chi)$ and $F(\chi)$ are expressed as power series in χ, the coefficients of which are to be determined. ϕ is a slowly varying function of χ. Here ϕ is taken as a constant and $F = a_1 + a_2\chi + a_3\chi^2$. Because Λ is an even function of χ, $a_2 = 0$ and

$$d^2\Lambda/d\chi^2 = \Lambda^2 - \chi^2 = a_4 \exp(-a_3\chi^2).$$

The zero moment of this equation over $0 \leqslant \chi \leqslant \infty$ yields in the light of $(d\Lambda/d\chi)_{\chi=0} = 0$ and $(d\Lambda/d\chi)_{\chi\to\infty} = 1$, $a_3 = \frac{1}{2}a_4^2\pi$. Also,

$$\Lambda^2(0) = a_4,$$

where $\Lambda(0) = 0{\cdot}8657$ (from the exact numerical solution). Thus

$$\Lambda = \{\chi^2 + 0{\cdot}7494 \exp(-0{\cdot}5886\chi^2)\}^{\frac{1}{2}}.$$

The author wishes to acknowledge with gratitude many very helpful and stimulating discussions with Profs G. F. Carrier and H. W. Emmons, who suggested the problem. He is also grateful for digital and analogue computer time furnished by Harvard University and the Missile Systems Division of Raytheon Company. This work was supported in the main by Nonr Contract 1866(34), administered by Prof. G. D. Birkhoff.

Partial list of symbols

a	scale factor in inviscid incompressible axisymmetric stagnation flow, time^{-1}
b	stoichiometric coefficient of oxidant
$\bar{B}$	frequency factor in Arrhenius kinetics, here (volume/time mole)
C_P	effective heat capacity at constant pressure for a gas mixture
D	mass transfer coefficient (binary diffusion coefficient) of Fick's law (area/time)
D_1	first Damkohler similarity group, here $\rho b d \bar{B}/2am$
d	stoichiometric coefficient of fuel
F	fuel
h	specific enthalpy
h_0	specific enthalpy of formation at some reference temperature T_0
Δh_c	$\Delta H_c/dm_F$
ΔH_c	specific heat released by combustion
L	differential operator
$\bar{L}$	heat of vaporization (or sublimation)/heat of combustion
Le	Lewis–Semenov number, D/χ
m	$\sum_{K=1}^{n} m_K \nu_1^K = \sum_{K=1}^{n} m_K \nu_2^K$
m_K	molecular weight of species K, mass of K/mole of K
M_K	molar concentration of K, moles of K/volume
n	total number of species present
O	oxidant
p	stoichiometric coefficient for the product
P	pressure or product

r radial co-ordinate $\bar{r} = (a/D)^{\frac{1}{2}}r$
(r.r.) reaction rate (moles/vol. sec)
T temperature $\bar{T} = T/(\Delta h_c/\alpha_F m_F)$
u radial component of velocity
$\mathbf{v}$ macroscopic velocity of mixture
w axial component of velocity
Y_K mass fraction of species K, ρ_K/ρ
$\bar{Y}_K$ stoichiometrically adjusted mass fraction of species K, $\alpha_K Y_K$
z axial co-ordinate $\bar{z} = (2a/D)^{\frac{1}{2}}\bar{z}$

Greek symbols

α_K $m/[(v_1^K - v_2^K)m_K]$
ϵ D_1^{-1} in § 9 and $D_1 \exp(-\bar{\theta}/\bar{T}_\infty)$ in § 8
η $(\bar{z} - \bar{z}_*)\epsilon^{-\frac{1}{3}}$ where $\epsilon = D_1^{-1}$
$\bar{\theta}$ $\theta/(\Delta h_c/\alpha_F m_F)$ where θ is the activation temperature of Arrhenius kinetics
Λ solution of a boundary-value problem arising for large D_1
λ thermal conductivity of Fourier's law
ν_1^K stoichiometric coefficient of the reactant K
ν_2^K stoichiometric coefficient of the product K
ξ a function of ϵ used in matching expansions
ρ $\sum_{K=1}^{n} \rho_K$ where ρ_K is the density of species K
χ an independent variable related to η; also, thermometric conductivity
ψ stream-function
ω_K mass rate of production of species K (mass of K/vol. time)

Subscripts and superscripts

d downstream outer expansion
F fuel
i inner expansion
K any species present
M maximum
O oxidant
P product
u upstream outer expansion
w two-phase interface
— non-dimensionalized or stoichiometrically adjusted
ξ intermediate variable used in matching expansions

REFERENCES

AGAFANOVA, F. A., GUREVICH, M. Q. & PALIEV, I. I. 1958 *Soviet Phys.-Tech. Phys.* **2**, 169.

BURKE, S. P. & SCHUMANN, T. E. W. 1928 *Industr. Engng Chem.* **20**, 998.

CHAMBRE, P. I. 1956 *J. Chem. Phys.* **25**, 417.

CHIN, C. L. D. 1962 A theoretical study of stagnation point region diffusion flames. Unpublished report submitted to the Division of Engineering and Applied Physics, Harvard University.

DOOLEY, D. A. 1956 Combustion in laminar mixing regions and boundary layers. Ph.D. thesis, California Institute of Technology.

FENDELL, F. E. 1964 Ignition and extinction in comb ustion of initially unmixed reactants Ph.D. thesis, Harvard University.

LENARD, M. 1962 Gas dynamics of chemically-reacting gas mixtures near equilibrium. *General Electric Space Sciences Laboratory Document* R 62 SD 985.

LINAN, A. 1963 On the structure of laminar diffusion flames. Ph.D. thesis, California Institute of Technology.

LORELL, J., WISE, H. & CARR, R. E. 1956 *J. Chem. Phys.* **25**, 325.

MARBLE, F. E. & ADAMSON, Jr., T. C. 1954 *Selected Combustion Problems*, pp. 111–31. London: Butterworth Scientific Publications.

NACHBAR, W., WILLIAMS, F. & PENNER, S. S. 1959 *Quart. Appl. Math.* **17**, 43.

SPALDING, D. B. 1954 *Fuel*, **33**, 255.

SPALDING, D. B. 1961 *J. Amer. Rocket Soc.* **31**, 763.

SPALDING, D. B. & JAIN, V. K. 1962 *Combustion and Flame*, **6**, 265.

ZELDOVITCH, Y. B. 1951 On the theory of combustion of initially unmixed gases. *NACA TM* 1296.